Closed-form analysis of thin radially polarized piezoelectric ceramic cylindrical shells with loss

D. D. Ebenezer* and Pushpa Abraham

Naval Physical and Oceanographic Laboratory, Kochi 682 021, India

Closed-form solutions to the equations of motion of radially polarized, piezoelectric, thin cylindrical shells derived using Kirchhoff's hypothesis are presented. The axial and radial components of displacement are expressed as sums of finite number of weighted exponential terms. Internal losses are represented by complex piezoelectric coefficients. The weights are determined using boundary conditions at the ends of the cylinder of finite length. The effect of the dimensions of the cylinder and the piezoelectric coefficients on the input electrical admittance is numerically investigated. The real and imaginary parts of all four piezoelectric coefficients used in the model have significant effect on the admittance. The investigation indicates that the inverse problem can be solved, i.e. the complex piezoelectric coefficients can be determined using the measured admittance.

PIEZOELECTRIC, ceramic cylindrical shells are often used in underwater sound navigation and ranging (sonar) transducers[1,2]. Axially polarized shells are used in Tonpilz (a German word meaning singing mushroom)[2] projectors and radially polarized shells are used in hydrophones. Projectors and hydrophones are underwater analogues of loud speakers and microphones respectively. Models of piezoelectric shells are necessary not only to model transducers, but also to determine the material properties of the shells. In this article a closed-form solution is presented for the equations of motion and boundary conditions[3] of thin, electrically excited, radially polarized, piezoelectric cylindrical shells. The effect of the dimensions of the shell and the piezoelectric coefficients on the input electrical admittance is investigated to see whether the model can be used for characterization.

Material properties of piezoelectric shells have significant variation, even when they are made in one batch. This causes a variation in the characteristics of transducers. Variations in the sensitivities of the hydrophones in a sonar array affect the accuracy of estimates of the direction of arrival of signals. It is, therefore, necessary to identify and use only those shells whose properties do not vary significantly from the mean properties of all the shells.

*For correspondence. (e-mail: tsonpol@vsnl.com)

Material properties are determined as follows: First, a model is used to obtain theoretical expressions for quantities that can be measured easily. These expressions will be functions of dimensions and material properties. Quantities that can be measured easily in the case of piezoelectric shells are, for example, the frequencies at which resonances and anti-resonances occur when the shell is electrically excited. Next, those quantities for which theoretical expressions were derived, and the dimensions, are measured and substituted in the theoretical expressions. Finally, the resulting equations are solved to find the material properties.

The equations to be solved are often transcendental and, furthermore, have to be solved simultaneously. The accuracy with which material properties can be determined therefore depends on measurement errors, the assumptions used to derive the theoretical model and errors in solving the equations. It is much more difficult to completely characterize piezoelectric ceramics than isotropic elastic material, because ten coefficients are to be determined in the former and only two in the latter.

In an earlier effort, a membrane model[4] of radially polarized cylindrical shells was used to determine[5] the real parts of four out of the ten coefficients. Later, a thin-shell model that includes the effect of bending stress and, therefore, better than the membrane model, was developed[3]; but an eigenfunction method was used to solve the governing equations and boundary conditions. The model can, in principle, be used to find the real parts of four coefficients. However, imaginary parts of the coefficients represent losses in the cylinder and cannot be determined by using the eigenfunction method.

The closed-form solution presented here has two advantages. First, axial and radial displacements, input electrical admittance and other functions are expressed as the sum of a finite number of terms and there is, therefore, no truncation error associated with the evaluation of these functions. Second, it is not based on eigenfunctions or free modes of vibration that do not exist when internal losses are present. Here, losses are represented by complex material properties and the response of the shell is finite even at resonance. In the lossless case, the response is infinite at resonance. Numerical results are also presented. First, it is shown that the complex admittance of a shell, with loss, obtained using the closed-form solution

is in good agreement with that obtained using 3D equations and ATILA[6] – a finite element program. This indicates that the assumptions made to derive the equations of motion are reasonable for thin shells. Next, the dependence of the input electrical admittance on the dimensions and material properties of the shell is investigated. The results indicate that it is possible to use the thin-shell model and the solution presented here to determine the complex material properties.

Theory

Consider a radially polarized, piezoelectric, ceramic cylindrical shell shown in Figure 1. The length of the shell is L, the mean radius is a, and the wall thickness is h. The inner and outer curved surfaces are completely electroded. The response of the cylinder to an applied voltage V is of interest. Specifically, the dependence of the complex input electrical admittance on the dimensions and complex material properties of the cylinder is of interest.

The strain–displacement relations of a thin, piezoelectric cylindrical shell are approximately expressed, by making use of Kirchhoff's hypothesis, in cylindrical coordinates as

$$S_\theta(r, z, \omega) = W(r, z, \omega)/(a+x) \cong W(a, z, \omega)/a, \quad (1)$$

and

$$S_z(r, z, \omega) = \partial U(a, z, \omega)/\partial z - x\partial^2 W(a, z, \omega)/\partial z^2, \quad (2)$$

where U and W are the radial and axial displacement respectively, $x = r-a$, S_θ and S_z are the normal strain in the θ and z directions respectively, and ω denotes angular frequency. The term containing x in eq. (2) is used to account for bending strain. It is neglected when using the membrane approximation.

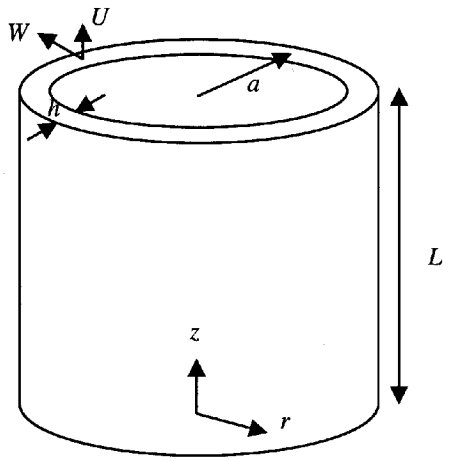

Figure 1. A thin, radially polarized, piezoelectric, ceramic shell of length L, average radius a, and wall thickness h. The inner and outer curved surfaces are completely electroded.

Because the shell is thin, and it has been assumed that Kirchhoff's hypothesis is valid, all stresses that are zero on the curved surfaces are assumed to be zero everywhere in the cylinder. Therefore, the piezoelectric equations of state are expressed[3] as

$$T_z(r, z, \omega) = \frac{1}{s_{11}^E(1-\sigma^2)}[S_z(r, z, \omega) + \sigma S_\theta(r, z, \omega) - d_{31}(1+\sigma)E_r(r, z, \omega)], \quad (3)$$

$$T_\theta(r, z, \omega) = \frac{1}{s_{11}^E(1-\sigma^2)}[S_\theta(r, z, \omega) + \sigma S_z(r, z, \omega) - d_{31}(1+\sigma)E_r(r, z, \omega)], \quad (4)$$

and

$$D_r(r, z, \omega) = d_{31}T_\theta(r, z, \omega) + d_{31}T_z(r, z, \omega) + \varepsilon_{33}^T E_r(r, z, \omega), \quad (5)$$

where

$$\sigma = -s_{12}^E / s_{11}^E, \quad (6)$$

T_θ and T_z are the normal stresses in the θ and z directions respectively, and D_r and E_r are the electric displacement and electric field respectively in the radial direction. The electroelastic coefficients s_{11}^E, s_{12}^E, d_{31} and ε_{33}^T have their usual definitions.

The electric displacement, D_r, must satisfy the electrostatic condition

$$\frac{1}{r}\frac{\partial}{\partial r}[rD_r(r, z, \omega)] = 0. \quad (7)$$

It is seen that

$$D_r(r, z, \omega) = D_0(a, z, \omega)/a, \quad (8)$$

is an approximate solution.

The electric field is assumed to vary linearly between the electrodes and is approximately expressed is

$$E_r(r, z, \omega) = V(\omega)/h + xE(z, \omega)/h, \quad (9)$$

where $V(\omega)$ is the applied voltage, and $E(z, \omega)$ has the dimensions of electric field and is to be determined.

It is seen that

$$D_r(r, z, \omega) = \frac{d_{31}}{s_{11}^E(1-\sigma)}\left[\frac{\partial}{\partial z}U(a, z, \omega) + \frac{1}{a}W(a, z, \omega)\right]$$

$$+\frac{\varepsilon_{33}^{T}(1-\sigma-2k_{31}^{2})}{1-\sigma}\frac{V(\omega)}{h}, \tag{10}$$

when

$$E(z,\omega)=\frac{hk_{31}^{2}}{d_{31}(1-\sigma-2k_{31}^{2})}\frac{\partial^{2}}{\partial z^{2}}W(a,z,\omega), \tag{11}$$

i.e. electric displacement is independent of radial coordinate and has the form shown in eq. (8), and the electrostatic condition is satisfied when E has the form shown in eq. (11).

Hamilton's principle can be used to obtain the equations of motion and boundary conditions. The equations of motion are[3]

$$[\Gamma]\begin{Bmatrix}U(a,z,\omega)\\W(a,z,\omega)\end{Bmatrix}-\rho h\omega^{2}\begin{Bmatrix}U(a,z,\omega)\\W(a,z,\omega)\end{Bmatrix}=\begin{Bmatrix}0\\CV(\omega)\end{Bmatrix}, \tag{12}$$

where

$$[\Gamma]=\frac{h}{a^{2}s_{11}^{E}(1-\sigma^{2})}\begin{bmatrix}-a^{2}\dfrac{\partial^{2}}{\partial z^{2}} & -\sigma a\dfrac{\partial}{\partial z}\\ \sigma a\dfrac{\partial}{\partial z} & 1+\beta^{2}(1+\varphi)a^{4}\dfrac{\partial^{4}}{\partial z^{4}}\end{bmatrix}, \tag{13}$$

$$\beta=\frac{h^{2}}{12a^{2}}, \tag{14}$$

$$\varphi=\frac{(1+\sigma)k_{31}^{2}}{1-\sigma-2k_{31}^{2}}, \tag{15}$$

$$k_{31}^{2}=\frac{d_{31}^{2}}{s_{11}^{E}\varepsilon_{33}^{T}}, \tag{16}$$

and

$$C=\frac{d_{31}}{as_{11}^{E}(1-\sigma)}. \tag{17}$$

The boundary conditions for free–free shells are[3]

$$\begin{bmatrix}\partial/\partial z & \sigma/a & -d_{31}(1+\sigma)/h\\ 0 & \partial^{2}/\partial z^{2} & 0\\ 0 & \partial^{3}/\partial z^{3} & 0\end{bmatrix}\begin{Bmatrix}U(a,z,\omega)\\W(a,z,\omega)\\V(\omega)\end{Bmatrix}=\begin{Bmatrix}0\\0\\0\end{Bmatrix},$$

$$z=0,L. \tag{18}$$

Equation (18) indicates that the axial force, shear force and bending moment are zero at the ends of the shell.

The solution to the equations of motion (eqs (12)–(17)) is expressed as

$$\begin{Bmatrix}U(a,z,\omega)\\W(a,z,\omega)\end{Bmatrix}=V(\omega)\begin{Bmatrix}\sum_{s=1}^{6}A_{s}e^{\lambda_{s}z}\\ \sum_{s=1}^{6}A_{s}\psi_{s}e^{\lambda_{s}z}+K\end{Bmatrix}, \tag{19}$$

where the frequency-dependent values of λ_s are the solutions to

$$\begin{vmatrix}-a^{2}\lambda_{s}^{2}-\Omega^{2} & -\sigma a\lambda_{s}\\ \sigma a\lambda_{s} & 1+\beta^{2}(1+\varphi)a^{4}\lambda_{s}^{4}-\Omega^{2}\end{vmatrix}=0, \tag{20}$$

$$\psi_{s}=-\frac{(a^{2}\lambda_{s}^{2}+\Omega^{2})}{\sigma a\lambda_{s}}=-\frac{\sigma a\lambda_{s}}{1+\beta^{2}(1+\varphi)a^{4}\lambda_{s}^{4}-\Omega^{2}} \tag{21}$$

$$\Omega^{2}=\omega^{2}a^{2}\rho\, s_{11}^{E}(1-\sigma^{2}), \tag{22}$$

and

$$K=\frac{ad_{31}(1+\sigma)}{h(1-\Omega^{2})}. \tag{23}$$

Equation (23) is obtained by substituting eq (19) in the second term in eq. (12) and equating the z-independent terms.

The weights, A_s, are determined by solving the equations obtained by substituting the expression for the displacements in eqs (19)–(23) in the six boundary conditions in eq. (18). Free–free shells are of interest for characterization purposes because the boundary conditions are easily achieved in practice. However, the weights are determined for other boundary conditions by using the same method.

Table 1. Material properties of piezoelectric ceramic

Material property	Value
ρ (kg/m^3)	7750
s_{11}^{E} (m^2/N)	$(16.4-j0.3)10^{-12}$
s_{12}^{E} (m^2/N)	$(-5.74+j0.1)10^{-12}$
s_{13}^{E} (m^2/N)	$(-7.22+j0.15)10^{-12}$
s_{33}^{E} (m^2/N)	$(18.8-j0.3)10^{-12}$
s_{44}^{E} (m^2/N)	$(47.5-j1)10^{-12}$
d_{31} (C/N)	$(-171+j3)10^{-12}$
d_{33} (C/N)	$(374-j7)10^{-12}$
d_{15} (C/N)	$(584-j10)10^{-12}$
$\varepsilon_{11}^{T}/\varepsilon_0$	$1730\,(1-j0.02)$
$\varepsilon_{33}^{T}/\varepsilon_0$	$1700\,(1-j0.02)$

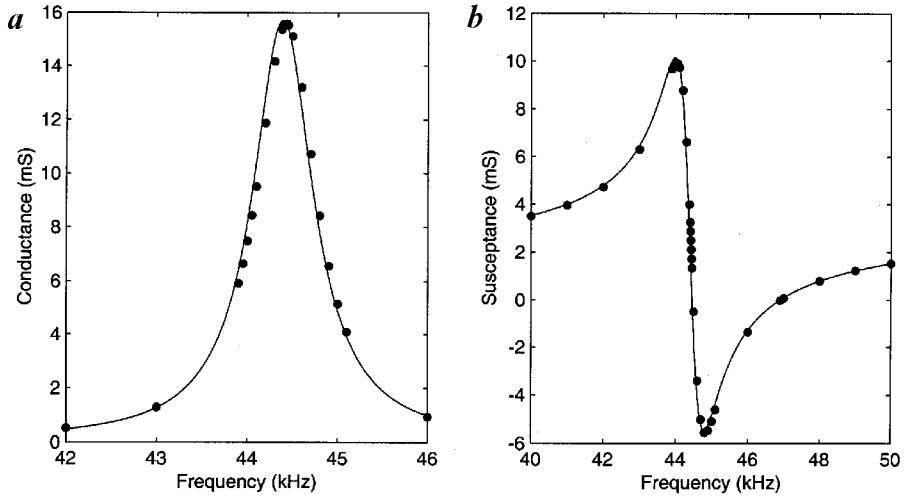

Figure 2. Input electrical (*a*) conductance and (*b*) susceptance of a shell with L = 10 mm, a = 10 mm and h = 1 mm in the neighbourhood of the first lower branch resonance frequency. Material properties are shown in Table 1. ——, Closed-form; •, ATILA.

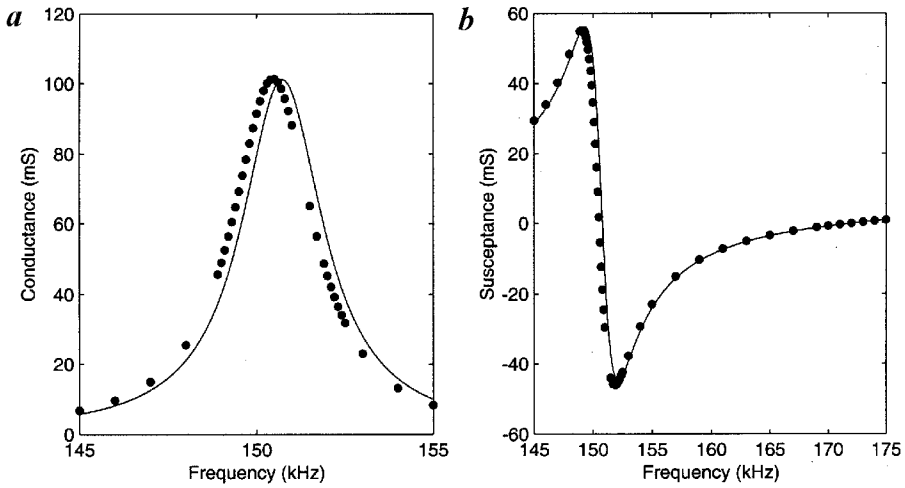

Figure 3. Input electrical (*a*) conductance and (*b*) susceptance of a shell with L = 10 mm, a = 10 mm and h = 1 mm in the neighbourhood of the first upper branch resonance frequency. Material properties are shown in Table 1. ——, Closed-form; •, ATILA.

Other functions of interest, such as strain and stress, are now obtained by substituting the values of A_s in the appropriate equations. The total charge

$$Q(\omega) = 2\pi a \int_0^L D_r(r, z, \omega)\mathrm{d}z, \tag{24}$$

on the surface of the electrodes is determined by substituting eqs (1) and (2) in eqs (3)–(6). It is expressed as

$$Q(\omega) = 2\pi a \int_0^L \left\{ \frac{d_{31}}{s_{11}^{\mathrm{E}}(1-\sigma)} \left[\frac{\partial U(a, z, \omega)}{\partial z} + \frac{W(a, z, \omega)}{a} - \frac{2d_{31}V(\omega)}{h} \right] + \varepsilon_{33}^{\mathrm{T}} \frac{V(\omega)}{h} \right\} \mathrm{d}z. \tag{25}$$

After substituting eqs (19)–(23) in eq. (25), the input electrical admittance,

$$Y(\omega) = j\omega Q(\omega)/V(\omega), \tag{26}$$

is expressed as

$$Y(\omega) = G(\omega) + jB(\omega) = j\omega 2\pi a \left\{ \frac{\varepsilon_{33}^{T} L}{h} \left(1 - \frac{2k_{31}^2}{1-\sigma} \right) \right.$$

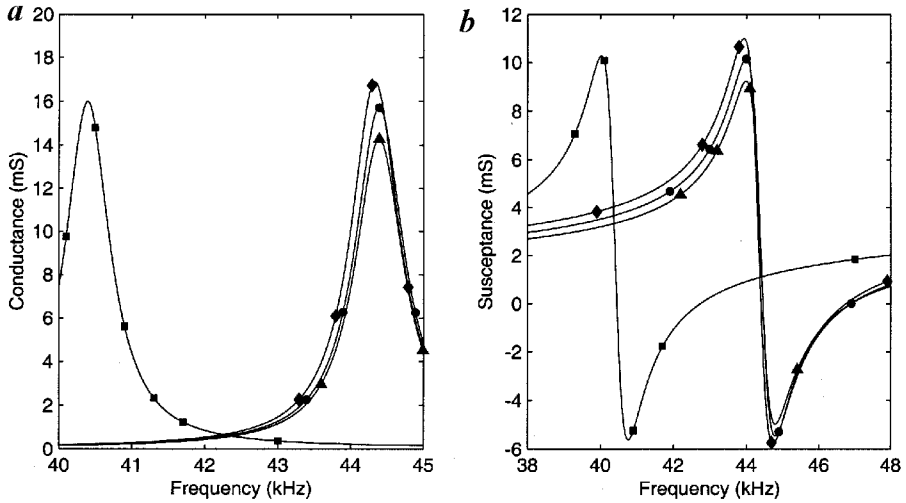

Figure 4. Input electrical (*a*) conductance and (*b*) susceptance of a shell in the neighbourhood of the first lower branch resonance frequency. Material properties are shown in Table 1. —●—, L = 10 mm, a = 10 mm and h = 1 mm; —◆—, L = 11 mm, a = 10 mm and h = 1 mm; —■—, L = 10 mm, a = 11 mm and h = 1 mm; —▲—, L = 10 mm, a = 10 mm and h = 1.1 mm.

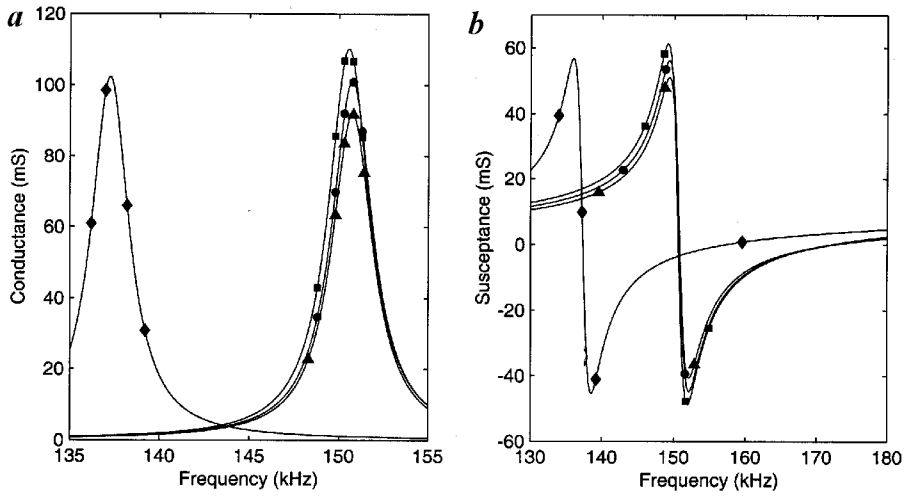

Figure 5. Input electrical (*a*) conductance and (*b*) susceptance of a shell in the neighbourhood of the first upper branch resonance frequency. Material properties are shown in Table 1. Other details as in Figure 4.

$$+\frac{d_{31}}{s_{11}^{\mathrm{E}}(1-\sigma)}\left[\frac{KL}{a}+\sum_{s=1}^{6}\left(\frac{A_{\mathrm{s}}\psi_{\mathrm{s}}\mathrm{e}^{\lambda_s L}}{a\lambda_{\mathrm{s}}}+A_{\mathrm{s}}(\mathrm{e}^{\lambda_s L}-1)\right)\right]\Bigg\}, \quad (27)$$

where $G(\omega)$ and $B(\omega)$ are the input electrical conductance and susceptance respectively.

Numerical results

Numerical results are now presented for thin, radially polarized, cylindrical shells. Unless otherwise mentioned, the material properties used in the computation are those shown in Table 1, and the dimensions of the shell are L = 100 mm, a = 10 mm and h = 1 mm. The real parts of the material properties are those of PZT5A (ref. 2) and the imaginary parts satisfy the conditions derived by Holland[7]. It is noted that only the coefficients $s_{11}^{\mathrm{E}}, s_{12}^{\mathrm{E}}, d_{31}$ and $\varepsilon_{33}^{\mathrm{T}}$ are used in the present model. However, all the ten coefficients are used in ATILA[6]. In ATILA, exact 3D governing equations are solved using axisymmetric, isoparametric, quadratic, finite elements.

The complex input electrical admittance of a shell, in the neighbourhood of the first resonance in the lower and upper branches, is shown in Figures 2 and 3 respectively. A solid line and dots are used to show the values computed using the closed-form solution and ATILA respectively. At the first resonance of both the branches, the

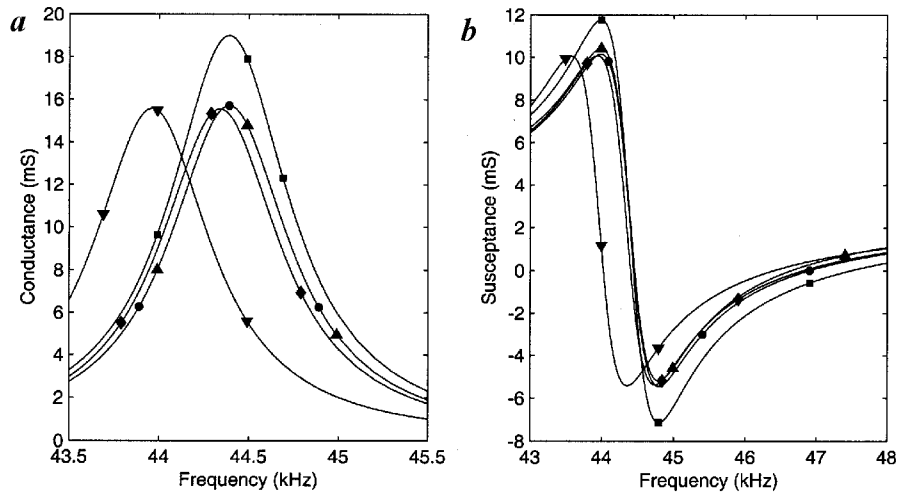

Figure 6. Input electrical (*a*) conductance and (*b*) susceptance of a shell in the neighbourhood of the first lower branch resonance frequency. Material properties are shown in Table 1, except for the following changes. —●—, No change; —▼—, $s_{11}^{E} = (16.4 \times 1.02 - j0.3)10^{-12}$; —◆—, $s_{12}^{E} = (-5.74 \times 1.1 + j0.1)10^{-12}$; —■—, $d_{31} = (-171 \times 1.1 + j3)10^{-12}$; —▲—, $\varepsilon_{33}^{T} / \varepsilon_0 = 1700(1.1 - j0.02)$.

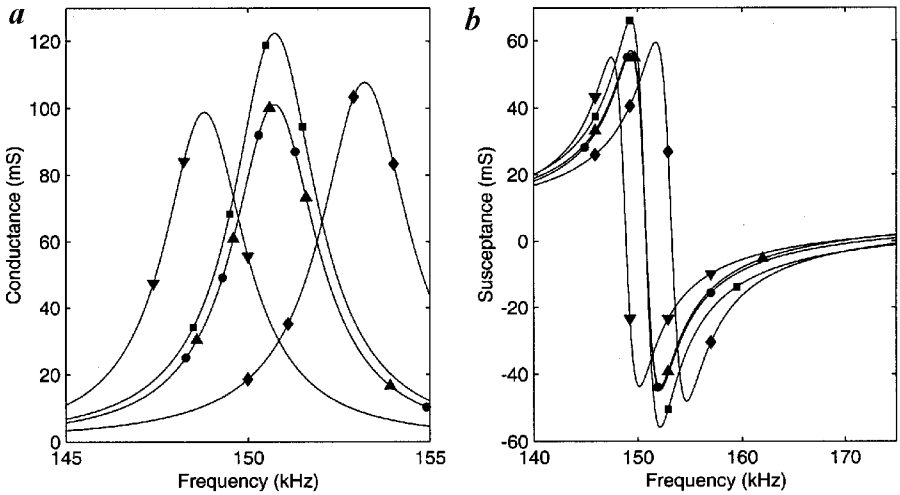

Figure 7. Input electrical (*a*) conductance and (*b*) susceptance of a shell in the neighbourhood of the first upper branch resonance frequency. Other details as in Figure 6.

radial displacement has no nodal point and the axial displacement has one nodal point. Therefore, the displacement distribution is similar at both resonances. However, in the lower branch, the maximum radial displacement is greater than the maximum axial displacement, and, in the upper branch, it is vice versa.

Even though several assumptions have been made to derive the equations of motion in the thin-shell model, it is seen from Figures 2 and 3 that the agreement is quite good. The resonance frequencies f_s^l in the lower branch and f_s^u in the upper branch, at which the input electrical conductance, G, is locally maximum; the locally maximum values of G; the frequencies at which the input electrical susceptance, B, is locally maximum; the locally maximum values of B; the frequencies at which B is locally minimum; the locally minimum value of B; and the anti-resonance frequencies f_p^l and f_p^u at which B becomes zero (about 47 kHz in Figure 2 *b* and 172 kHz in Figure 3 *b*), are all in good agreement. This is of interest because measured values of these frequencies can be used for characterization[5].

The effect of changes in the dimensions of the shell is shown in Figures 4 and 5. The complex admittances of shells with the following dimensions are shown: L = 10 mm, a = 10 mm and h = 1 mm; L = 11 mm, a = 10 mm and h = 1 mm; L = 10 mm, a = 11 mm and

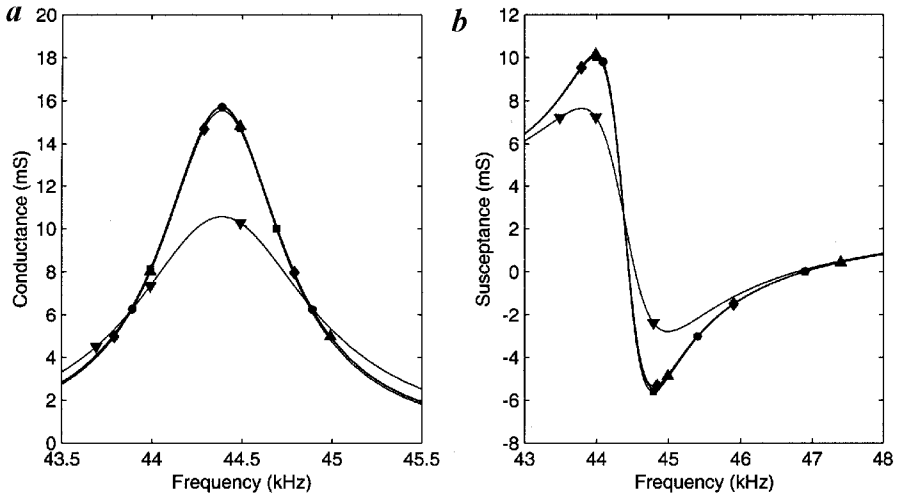

Figure 8. Input electrical (*a*) conductance and (*b*) susceptance of a shell in the neighbourhood of the first lower branch resonance frequency. Material properties are shown in Table 1, except for the following changes. —●—, No change; —▼—, $s_{11}^{E} = (16.4 - j0.3 \times 1.5)10^{-12}$; —◆—, $s_{12}^{E} = (-5.74 + j0.1 \times 1.5)10^{-12}$; —■—, $d_{31} = (-171 + j3 \times 1.5)10^{-12}$; —▲—, $\varepsilon_{33}^{T} / \varepsilon_0 = 1700(1 - j0.02 \times 1.5)$.

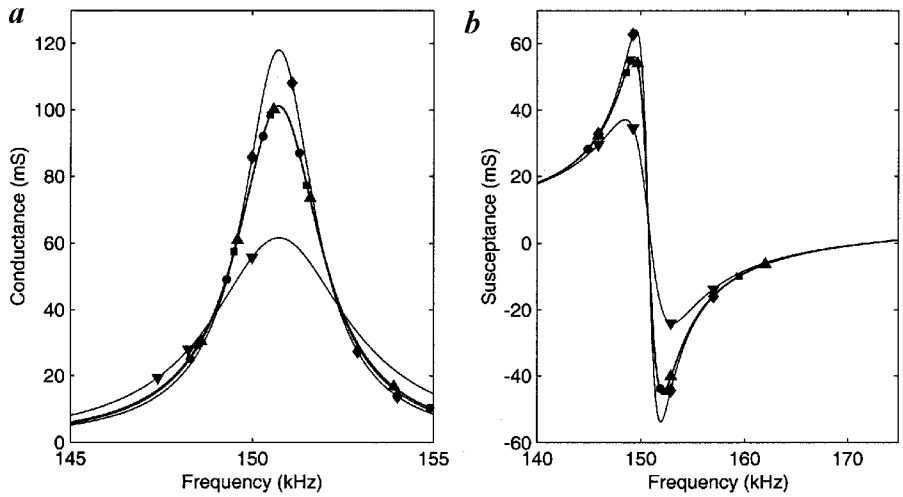

Figure 9. Input electrical (*a*) conductance and (*b*) susceptance of a shell in the neighbourhood of the first upper branch resonance frequency. Other details as in Figure 8.

h = 1 mm; and L = 10 mm, a = 10 mm and h = 1.1 mm. It can be seen from Figures 4 and 5 that the mean radius, a, has a strong effect on the lower branch resonance frequency, f_s^l, and the length, L, has a strong effect on the upper branch resonance frequency, f_s^u. The thickness, h, does not have a strong effect on either resonance frequency.

The effect of increasing the real part of s_{11}^{E} by 2% and the real parts of the s_{12}^{E}, d_{31}, and ε_{33}^{T} by 10%, one at a time, is shown in Figures 6 and 7 in the neighbourhoods of f_s^l and f_s^u respectively. The values shown in Figures 2 and 3 for a cylinder of L = 10 mm, a = 10 mm and h = 1 mm are also shown in Figures 6 and 7 respectively to make the comparison easier. It can be seen from Figures 6 and 7 that the real part of s_{11}^{E} has a strong effect on f_s^l and f_s^u. The real part of s_{12}^{E} has a strong effect on f_s^u and a lesser effect on f_s^l. The real part of d_{31} does not have a strong effect on the resonance frequencies, but only on the values of G at these frequencies. It also has a strong effect on the anti-resonance frequencies, f_p^l and f_p^u, in the lower and upper branches respectively. The real part of ε_{33}^{T} does not have a strong effect on the admittance in the frequency regions shown in Figures 6 and 7, but has a strong effect on the input electrical susceptance B, at frequencies that are much lesser than all resonance frequencies.

The effect of increasing the imaginary parts of s_{11}^{E}, s_{12}^{E}, d_{31} and ε_{33}^{T}, one at a time, by 50%, is shown in Figures 8 and 9. It is verified that the conditions in Holland[7] are satisfied after increasing the coefficients. It is seen from Figure 8 that only the imaginary part of s_{11}^{E} has a strong effect on G and B in the neighbourhood of f_s^{l}. Changes in the imaginary parts of the other coefficients have lesser effect. It is seen from Figure 9 that only the imaginary parts of s_{11}^{E} and s_{12}^{E} have a strong effect on G and B in the neighbourhood of f_s^{u}. The imaginary part of d_{31} has a weak effect on the locally maximum value of B. The imaginary part of ε_{33}^{T} has an effect on the values of G at low frequencies, but this is not shown in the figures. The effect of the imaginary parts of the coefficients on the input electrical admittance is also investigated using ATILA, and the conclusions are the same.

Conclusions

A closed-form solution to the equations governing electrically excited, thin, radially polarized, cylindrical shells with loss is presented. Expressions for all quantities of interest are sums of a finite number of terms, and there is no truncation error associated with evaluation of infinite series. For thin shells, the numerical results are in good agreement with those obtained using ATILA.

The effect of dimensions and piezoelectric coefficients on the input electrical admittance in the neighbourhood of resonance frequencies is numerically investigated. The study shows that the real and imaginary parts of s_{11}^{E}, s_{12}^{E}, d_{31} and ε_{33}^{T} have an effect on the input electrical admittance at low frequencies or in the neighbourhoods of the first resonance frequency in the lower and upper branches. It may therefore be possible to determine these coefficients using measured values of admittance.

1. Stansfield, D., *Underwater Electroacoustic Transducers*, Bath University Press, Bath, 1990.
2. Wilson, O. B., *Introduction to the Theory and Design of Sonar Transducers*, Peninsula Publishing, Los Altos, CA, 1988.
3. Ebenezer, D. D. and Abraham, P., *J. Acoust. Soc. Am.*, 1999, **105**, 154–163.
4. Haskins, J. F. and Walsh, J. I., *ibid*, 1957, **29**, 729–734.
5. Ebenezer, D. D. and Sujatha, A. J., *ibid*, 1997, **102**, 1540–1548.
6. Decarpigny, J.-N., Debus, J.-C., Tocquet, B. and Boucher, D., *ibid*, 1985, **78**, 1499–1507.
7. Holland, R., *IEEE Trans. Sonics Ultrason.*, 1967, **14**, 18–20.

ACKNOWLEDGEMENT. Permission from the Director, Naval Physical and Oceanographic Laboratory, Kochi to publish this article is gratefully acknowledged.

Received 6 May 2002; revised accepted 26 July 2002